

Electron-Electron Interactions and Plasmon Dispersion in Graphene

L. S. Levitov

Massachusetts Institute of Technology, 77 Massachusetts Avenue, Cambridge MA 02139, USA

A. V. Shtyk and M. V. Feigelman

L. D. Landau Institute for Theoretical Physics, Kosygin str. 2, Moscow, 119334 Russia

Plasmons in two-dimensional systems with non-parabolic band, such as graphene, feature strong dependence on electron-electron interactions. We use a many-body approach to relate plasmon dispersion at long wavelengths to the Landau's Fermi-liquid interaction parameters and quasiparticle velocity. This general relation is illustrated using a model with N fermion species, giving a power-law dependence for plasmon frequency vs. carrier density at leading order in large N . An identical renormalization is predicted for magnetoplasmon resonance. We propose that gate-tunability of plasmons in graphene can be used to directly probe the effects of electron-electron interaction.

Plasmonics has emerged recently as an active direction in graphene research¹⁻⁵. Surface plasmons in 2D electron systems are propagating charge density waves in which collective dynamics of clouds of charge is mediated by electric field in 3D.⁶ The dual matter-field nature of plasmons is a key ingredient for many interesting and important phenomena^{7,8}. Plasmons in graphene display a range of potentially useful properties, such as low Ohmic losses, a high degree of field confinement, and gate-tunability, which make these excitations of great interest for optoelectronics^{9,10}. Gate-tunability of plasmons in graphene was demonstrated recently^{11,12}.

The goal of this article is to relate the density dependence of plasmons with the interactions in the electron system. Plasmon dispersion depends on carrier density due to several effects. It takes simplest form in the limit of a weak electron-electron interaction,¹⁻⁴

$$\omega^2 = \frac{2e^2 E_F}{\kappa \hbar^2} q \quad (1)$$

where $E_F \sim n^{1/2}$ is the Fermi energy of noninteracting massless Dirac particles, and n is carrier density. Here κ is an effective dielectric constant of the substrate and a long-wavelength limit is assumed, $q \ll p_F$. Interestingly, plasmon dispersion is also affected by interactions. Renormalization of the ω vs. q relation, Eq.(1), due to the effects of electron-electron interaction was predicted in Ref.13, where perturbation expansion in a weak fine structure parameter $\alpha = e^2/\hbar v$ was employed. The results of Ref.13 point to an interesting possibility to directly probe the effects of electron interactions by measuring plasmon dispersion relation. However, because of strong interactions in graphene, $\alpha \sim 2.5$, the weak coupling approximation cannot serve as a good model, and a different approach is required.

Acknowledging the difficulty of modelling the strong-coupling regime, it is beneficial to approach the problem at a somewhat more general angle. Rather than attempting to make predictions based on a specific microscopic models, one can ask if a relation between the dispersion and some other fundamental characteristics of the system can be established. Below we point out that such

a relation arises naturally from the Landau theory of Fermi liquids.¹⁴ This theory affords a general, model-independent framework to describe systems of strongly interacting fermions at degeneracy. The effects of interactions are described by Landau parameters, representing a "genetic code" of the Fermi liquid (FL). Their values can in principle be predicted from perturbation theory if interactions are weak. For systems with strong interactions, however, the most reliable way to obtain the Landau parameters is to use their relation with experimentally measurable quantities, such as compressibility, heat capacity, spin susceptibility and dispersion of collective excitations.

Our many-body analysis upholds the conventional square-root dependence $\omega \sim q^{1/2}$. We show that all the effects of interactions are accumulated in the prefactor,

$$\omega^2 = Y \lambda q, \quad Y = (1 + F_1)v, \quad \lambda = \frac{N e^2 p_F}{2 \kappa \hbar^2} \quad (2)$$

where p_F is Fermi momentum, $N = 4$ is the number of spin/valley flavors, and a long-wavelength limit is assumed, $q \ll p_F$. Here F_1 is the Landau interaction harmonic with $m = 1$, and v is the Fermi velocity renormalized by interactions. The dielectric constant κ may have a q dependence describing image charges arising due to conducting boundaries such as gates. In this case, a simple model $\kappa(q) = \frac{1}{2}(\epsilon_1 + \epsilon_2 \coth(qd))$ yields an acoustic plasmon dispersion $\omega \sim q$.¹⁵ The quantity λ in Eq.(2) has units of frequency and depends only on the fundamental constants and carrier density via p_F .

Magnetic field turns the gapless plasmon mode into a gapped mode. The magnetoplasmon dispersion relation obtained by adding Lorentz force to the Landau FL dynamics takes the following form:

$$\omega_B^2(q) = \omega_0^2(q) + Y^2 (eB/cp_F)^2 \quad (3)$$

where $\omega_0(q)$ is plasmon dispersion at $B = 0$ given by Eq.(2). The size of the gap at $q = 0$ scales linearly with B , with the prefactor that varies inversely with $p_F \sim n^{1/2}$. Notably, the magnetoplasmon dependence on the interactions is described by the same combination $Y = (1 + F_1)v$ as that appearing in Eq.(2).

The quantity Y governs the interaction dependence of plasmon dispersion. Measuring it as a function of carrier density can shed light on the role of electron-electron interactions in the system. This behavior is in sharp departure with that for plasmons in two-dimensional systems with parabolic band dispersion, where Galilean invariance leads to an identity for Landau parameters, $(1 + F_1)v = v_0$,¹⁴ where $v_0 = mp_F$ is Fermi velocity of noninteracting particles at the same density. As a result, the value $(1 + F_1)v$ is independent of interactions, leading to the “universal” long-wavelength plasmon dispersion in the parabolic case, $\omega_0^2(q) = \frac{2\pi e^2 n}{m\kappa(q)}q$ at $B = 0$ and $\omega_B^2(q) = \omega_0^2(q) + \omega_c^2$ for magnetoplasmon (where m is unrenormalized band mass and $\omega_c = eB/mc$ is the cyclotron frequency). These dependences carry no information on the quantum effects and neither on the interactions.

The situation is quite different in systems with non-parabolic dispersion, such as graphene. The density dependence in Y arises because the values v and F_1 depend on the phase volume of the states in the conduction band contributing to renormalization. The energies of these states span the domain from graphene bandwidth down to the Fermi energy, which is gate-tunable. To illustrate this point, we analyze the limit of a large number of spin/valley flavors, $N \gg 1$. In this case, as we will see, Eq.(2) yields a power-law dependence on carrier density, giving

$$\omega^2 \propto n^{(1-\beta)/2}q \quad (4)$$

with the exponent value identical to that found from one-loop RG analysis for velocity renormalization, $\beta = \frac{8}{N\pi^2}$.^{16–18} For a non-interacting system, $\beta = 0$. Crucially, the power law $n^{(1-\beta)/2}$ describes the dependence on carrier density not only near charge neutrality but also for all accessible n values.

Measurements of the density dependence of a plasmon resonance were reported in Ref.11. The observed dependence approximately follows the relation $\omega^2 \propto q$, with the prefactor exhibiting an approximately linear dependence on $n^{1/2}$. However, the range of densities in which the dispersion was measured was not wide enough to provide a clear distinction between $\beta = 0$ and $\beta \neq 0$. An attempt to experimentally determine the RG scaling exponents from transport measurements was made recently in Ref.19, where a systematic variation of the period of quantum oscillations with carrier density was interpreted in terms of Fermi velocity renormalization, giving a value $\beta = 0.5-0.55$. This value is considerably larger than the one-loop RG result, $\beta = \frac{8}{\pi^2 N} \approx 0.2$, see below. This discrepancy is not yet understood.

We note parenthetically that the interaction effects are not expected to vanish in graphene bilayer despite the parabolic character of its band dispersion. Electronic states in graphene bilayer are Dirac-like rather than Schrödinger like, and hence do not admit Galilean transformation. For plasmons in this material we there-

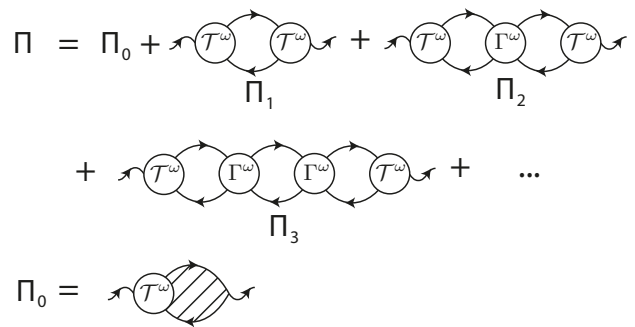


FIG. 1: Resummed Feynman graphs for the polarization operator $\Pi(\mathbf{q}, \omega)$. The non-quasiparticle contribution $\Pi_0(\mathbf{q}, \omega)$ and the FL ladder $\sum_{n \geq 1} \Pi_n(\mathbf{q}, \omega)$ are shown. Only the contributions $\Pi_1(\mathbf{q}, \omega)$ and $\Pi_2(\mathbf{q}, \omega)$ contribute to the low-energy plasmon dispersion, see text.

fore expect a behavior similar to that in materials with nonparabolic band, described by Eqs.(2),(3).

I. MICROSCOPIC FERMI-LIQUID ANALYSIS

The goal of this section is to relate plasmon dispersion with the standard quantities such as Landau FL interaction parameters and renormalized velocity. The analysis proceeds by standard steps via resumming the ladder contributions to the dynamical polarization function which account for the quasiparticle dynamics in Landau’s FL framework. This leads to a polarization response, $\Pi(q, \omega) \sim q^2/\omega^2$, describing plasmon excitations in the low-frequency and long-wavelength domain, $\omega \ll E_F$, $q \ll p_F$.

Charge carriers in graphene single layer are described by the Hamiltonian for $N = 4$ species of massless Dirac particles. In second-quantized representation the Hamiltonian reads

$$\mathcal{H} = \sum_{\mathbf{p}, i} \psi_{\mathbf{p}, i}^\dagger v_0 \boldsymbol{\sigma} \mathbf{p} \psi_{\mathbf{p}, i} + \mathcal{H}_{\text{el-el}}, \quad (5)$$

$$\mathcal{H}_{\text{el-el}} = \frac{1}{2} \sum_{\mathbf{q}, \mathbf{p}, \mathbf{p}', i, j} V(\mathbf{q}) \psi_{\mathbf{p}+\mathbf{q}, i}^\dagger \psi_{\mathbf{p}-\mathbf{q}, j}^\dagger \psi_{\mathbf{p}', j} \psi_{\mathbf{p}, i}, \quad (6)$$

where $i, j = 1 \dots N$, $v_0 \approx 10^6 \text{cm/s}$ is unrenormalized Fermi velocity, and $V(\mathbf{q}) = 2\pi e^2/|\mathbf{q}|\kappa$ is the Coulomb interaction with the dielectric constant κ describing screening by the substrate. Here $\psi_{\mathbf{p}, i}$ is a two-component spinor with the components describing the wavefunction amplitude on two sublattices of the graphene crystal lattice. The amplitudes associated with the two sublattices are usually referred to as pseudospin up and down components, with the (pseudo)spin-1/2 Pauli matrices in Eq.(5) acting on (pseudo)spinors $\psi_{\mathbf{p}, i}$.

Plasmons are collective excitations of 2D electrons coupled by the electric field in 3D. They can be described

microscopically using the density correlation function

$$K(\mathbf{q}, \omega) = \int dt \langle \rho_{\mathbf{q}}(t) \rho_{\mathbf{q}}(t_0) \rangle e^{i\omega(t-t_0)} \quad (7)$$

where $\rho_{\mathbf{q}}(t) = \sum_{\mathbf{p}, i} \psi_{\mathbf{p}, i}^\dagger(t) \psi_{\mathbf{p}+\mathbf{q}, i}(t)$ are Fourier harmonics of the total electron density. The quantity K is expressed in a standard fashion¹⁴ through geometric series involving the polarization function $\Pi(\mathbf{q}, \omega)$ defined as the irreducible density-density correlator,

$$K(\mathbf{q}, \omega) = \frac{\Pi(\mathbf{q}, \omega)}{\epsilon(\mathbf{q}, \omega)}, \quad \epsilon(\mathbf{q}, \omega) = 1 - V(\mathbf{q})\Pi(\mathbf{q}, \omega) \quad (8)$$

Zeros of the dynamical screening function $\epsilon(\mathbf{q}, \omega)$ give the poles of K , defining plasmon dispersion. To obtain the dispersion from the condition $\epsilon(\mathbf{q}, \omega) = 0$ we need to gain information on $\Pi(\mathbf{q}, \omega)$ from a microscopic approach. In the long-wavelength limit, $q \ll p_F$, $\omega \ll E_F$, the behavior of the quantity $\Pi(\mathbf{q}, \omega)$ is dominated by excitations near the Fermi surface, which can be described in the FL framework.

The microscopic approach which forms the basis of the FL phenomenology involves several standard steps. At a first step, we isolate the contribution due to the quasiparticle pole of the electron Greens function $G(x-x') = -i \langle \psi(x) \psi^\dagger(x') \rangle$ near the Fermi surface,

$$G(\epsilon, \mathbf{p}) = G^{(\text{reg})}(\epsilon, \mathbf{p}) + G^{(\text{sing})}(\epsilon, \mathbf{p}). \quad (9)$$

The first term is a regular part of the Greens function behaving as a smooth function near the Fermi level. The second term is a singular contribution describing quasiparticles, which dominates the FL dynamics:

$$G^{(\text{sing})}(\epsilon, \mathbf{p}) = \frac{Z}{i\epsilon - \xi(p) + i\gamma \text{sgn}\epsilon}. \quad (10)$$

Here Z is a quasiparticle residue, γ is a quasiparticle decay rate, and $\xi(p) = v(p-p_F)$ is a quasiparticle energy dispersion, with v the renormalized velocity.

This general relation can be specialized to the case of graphene as follows. The Green's function for electrons in graphene has a 2×2 matrix pseudospin structure. By projecting on the conduction and valence band, it can be represented as

$$\hat{G}(\epsilon, \mathbf{p}) = G_{<}(\epsilon, \mathbf{p}) \hat{P}_{<} + G_{>}(\epsilon, \mathbf{p}) \hat{P}_{>} \quad (11)$$

where $\hat{P}_{>(<)} = (1 \pm \boldsymbol{\sigma} \mathbf{e}_p)/2$ are projectors for the two bands (here \mathbf{e}_p is a unit vector in the direction of momentum \mathbf{p}). The quasiparticle excitations with low energies, which govern the low-frequency and long-wavelength response, reside near the Fermi level. Without loss of generality, we assume n-type doping, so that the Fermi level lies in the upper band, $E_F > 0$. In this case, excitations from the lower band do not appear explicitly in the FL theory and lead only to renormalization of various parameters such as the effective interactions and the quasiparticle velocity. The quasiparticle pole in Eq.(9)

therefore arises only from the upper-band contribution $G_{>}$ whereas the lower-band contribution $G_{<}$ can be absorbed into the regular part $G^{(\text{reg})}$. Below the subscripts $>$ and $<$ will be omitted for brevity.

The next step, which is key for understanding the role of low-energy excitations, is the analysis of the polarization function $\Pi(q, \omega)$ at small ω and q . This is done by identifying the contributions due to pairs of Greens functions with proximal poles (the ‘‘dangerous’’ two-particle crosssections),¹⁴ which we write symbolically as $G^{(\text{sing})}G^{(\text{sing})} \sim Z^2 \frac{\mathbf{v}\mathbf{k}}{\omega - \mathbf{v}\mathbf{k}}$. One can represent $\Pi(q, \omega)$ as a sum of terms with different numbers of such contributions,

$$\Pi(q, \omega) = \Pi_0(q, \omega) + \Pi_1(q, \omega) + \Pi_2(q, \omega) + \dots \quad (12)$$

$$\Pi_1(q, \omega) = \mathcal{T}^\omega G G \mathcal{T}^\omega, \quad \Pi_2(q, \omega) = \mathcal{T}^\omega G G \Gamma^\omega G G \mathcal{T}^\omega \dots$$

The corresponding graphs are shown in Fig.1. Here we introduced so-called quasiparticle-irreducible quantities: the renormalized scalar vertex \mathcal{T}^ω and the two-particle scattering vertex Γ^ω (see Fig.2 b,c). These quantities absorb all non-quasiparticle contributions in the upper band as well as the inter-band processes and the contribution of the states in the lower band.

We recall that the quasiparticle-irreducible quantities are distinct from the conventional irreducible quantities defined as sums of Feynman graphs that cannot be split in two by removing two electron lines¹⁴. For example, the quasiparticle-irreducible vertex Γ^ω is obtained by summing all kinds of graphs except the ones with dangerous cross-sections. The vertex Γ^ω (\mathcal{T}^ω) can be obtained from the conventional irreducible vertex Γ_0 (\mathcal{T}_0) by the resummation procedure pictured in Fig.2, where the hatched blocks represent contributions due to pairs of Greens functions save for $G^{(\text{sing})}G^{(\text{sing})}$.

To analyze the dependence on ω and \mathbf{q} in the long-wavelength limit, we exercise caution and employ the quantities \mathcal{T}^ω and Γ^ω taken at small but nonzero frequency and momentum values. We therefore adopt an approach similar to that used in Ref.20: our quasiparticle-irreducible quantities correspond to Luttinger's ω -quantities which are taken at finite ω and \mathbf{q} . They are distinct from the conventional ω -quantities¹⁴ obtained in the limit $\omega, q \rightarrow 0$, ($\omega \gg v_F q$). This distinction, however, turns out to be inessential: Luttinger's ω -quantities reproduce the conventional ω -quantities in the limit $\omega, q \rightarrow 0$, which can be taken in arbitrary order since dangerous cross-sections were left out of the definition of \mathcal{T}^ω and Γ^ω .

Proceeding with the analysis, we note that the dependence on ω and q is very different for $\Pi_0(q, \omega)$ and $\Pi_{n \geq 1}(q, \omega)$. We will first analyze the contribution $\Pi_0(q, \omega)$. This quantity does not contain dangerous cross-sections which can generate a nonanalytic behavior at small ω and \mathbf{q} . Taking $\Pi_0(q, \omega)$ to be analytic, we can represent it as

$$\Pi_0(\mathbf{q}, \omega) = A(\omega) + B(\omega) \left(\frac{q}{p_F} \right)^2 + \dots \quad (13)$$

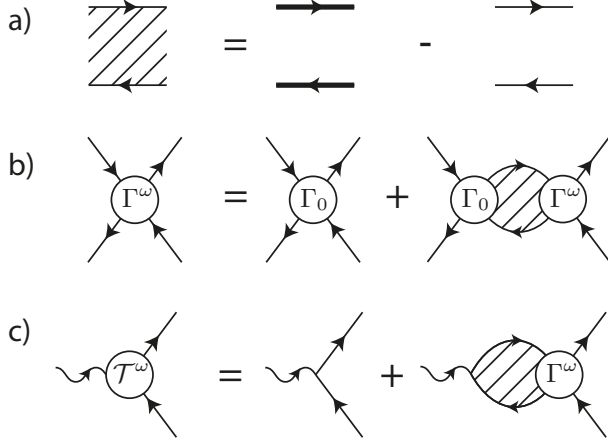


FIG. 2: Feynman graphs for the “quasiparticle-irreducible” quantities \mathcal{T}^ω , Γ^ω . Bold lines represent a full Green’s function while the thin lines corresponds to a singular part $G^{(\text{sing})}$. The vertex Γ_0 represents the conventional irreducible vertex, whereas hatched blocks represent products of two Green’s functions save for the contributions $G^{(\text{sing})}G^{(\text{sing})}$ which give a non-analytical behavior at small ω , \mathbf{q} , see text.

where $A(\omega)$ and $B(\omega)$ are regular functions. We recall that gauge invariance prohibits any physical response to spatially uniform time-dependent scalar field. Applying this to the full polarization function, Eq.(12), we conclude that setting $q = 0$ yields $\Pi(\omega, 0) = 0$. Also, since the contributions of the dangerous cross-sections GG vanish at $q = 0$, all the quantities $\Pi_{n \geq 1}(q, \omega)$ do so. We therefore conclude that the function $A(\omega)$ vanishes, leaving us with $\Pi_0(\mathbf{q}, \omega) = (q/p_F)^2 B(\omega) + O(q^4)$. This gives an effective q -dependent permittivity

$$\tilde{\kappa}(q, \omega) = 1 - V(q)\Pi_0(q, \omega). \quad (14)$$

Since $V(q) = 2\pi e^2/\kappa q$ in 2D, the effective long-wavelength permittivity is equal to unity and may henceforth be ignored in the limit $q/p_F \rightarrow 0$.

It is instructive to compare the behavior of $\tilde{\kappa}(q, \omega)$ with that arising for $q \gg p_F$. In this case the effects of finite doping are negligible and we can estimate the polarization function using the result obtained for massless Dirac particles at zero doping,

$$\Pi(q, \omega) = -\frac{N}{16} \frac{q^2}{\sqrt{q^2 v^2 - \omega^2}}, \quad (15)$$

where $N = 4$ is the number of spin/valley flavors. In the limit $qv \gg \omega$, we obtain a well known q -independent result for permittivity

$$\tilde{\kappa}(q, \omega) = 1 + \frac{\pi N \alpha}{8} \quad (16)$$

This expression describes the effect of intraband polarization in undoped graphene. We stress, however, that while the above expression is different from unity, it is obtained

for q and ω which are not relevant for plasmon excitations. In fact, plasmons do not exist for such $\Pi(\mathbf{q}, \omega)$, as the plasmon dispersion terminates for $q \gtrsim p_F$. At the same time, the permittivity found in the long-wavelength limit $q \ll p_F$, $\omega \ll E_F$, which is relevant for plasmons, equals unity.

Next, we proceed with the analysis of the remaining terms, $\Pi_{n \geq 1}(q, \omega)$, which contribute to the low-energy plasmon dispersion. This is the part of polarization which account for the quasiparticle contributions. The corresponding Feynman graphs are given by a ladder with rungs consisting of two quasiparticle lines separated by vertex parts, as shown on a Fig.1. This gives geometric series that can be easily summed up:

$$\Pi(\mathbf{q}, \omega) = N \oint \frac{d\theta}{2\pi} \mathcal{T}^\omega \left(\frac{\nu Z^2}{\omega - \mathbf{q}\mathbf{v}(1 + \hat{F})} \mathbf{q}\mathbf{v}\mathcal{T}^\omega \right), \quad (17)$$

where \hat{F} is an integral operator

$$\hat{F}f(\theta) = \nu Z^2 \oint \frac{d\theta'}{2\pi} \Gamma^\omega(\omega, \mathbf{q}, \theta, \theta') f(\theta'). \quad (18)$$

Here $\nu = p_F/(2\pi\hbar^2 v)$ is density of states per flavor, θ is an angle between \mathbf{p} and \mathbf{q} . For zero external momentum $\mathbf{q} \rightarrow 0$ the kernel of the operator \hat{F} depends only on the angle between \mathbf{p} and \mathbf{p}' . In fact, we will need only the quantity $\Gamma^\omega(0, 0, \theta, \theta') \equiv \Gamma^\omega(\theta - \theta')$.

The scalar vertex \mathcal{T}^ω on the Fermi surface with small external frequency and momentum ω , $v_F q \ll \varepsilon_F$ can be decomposed as

$$\mathcal{T}^\omega(\omega, \mathbf{q}, \theta) = \mathcal{T}_0 + \mathcal{T}_1 \omega + \mathcal{T}_2 q \cos \theta + \dots \quad (19)$$

where $\mathcal{T}_0 = Z^{-1}$ by virtue of Ward’s identity¹⁴. The linear terms might have been important, if assessed by power counting. However these contributions drop out, because for external frequency ω and momentum \mathbf{q} , the expressions in question contain both $\mathcal{T}^\omega(\omega, \mathbf{q}, \theta)$ and $\mathcal{T}^\omega(-\omega, -\mathbf{q}, \theta)$. This leads to a cancellation of the terms linear in ω and \mathbf{q} .

In fact, only first two terms of these series are relevant for long-wavelength plasmons with $v_F q \ll \omega \ll \varepsilon_F$. Anticipating the square root dependence for plasmon frequency vs. wavenumber, we expand in qv/ω to obtain

$$\begin{aligned} \Pi_1 &= \oint \frac{d\theta}{2\pi} \mathcal{T}^\omega(\omega, \mathbf{q}, \theta) \frac{\nu Z^2 v q \cos \theta}{\omega - v q \cos \theta} \mathcal{T}^\omega(-\omega, -\mathbf{q}, \theta) \\ &= \nu Z^2 \mathcal{T}_0^2 \oint \frac{d\theta}{2\pi} \frac{(v q \cos \theta)^2}{\omega^2} = \frac{\nu v^2 q^2}{2 \omega^2}, \end{aligned} \quad (20)$$

$$\begin{aligned} \Pi_2 &= \oint \frac{d\theta d\theta'}{(2\pi)^2} \mathcal{T}^\omega(\omega, \mathbf{q}, \theta) \frac{\nu Z^2 v q \cos \theta}{\omega} \Gamma^\omega(\omega, \mathbf{q}, \theta, \theta') \\ &\quad \times \frac{\nu Z^2 v q \cos \theta'}{\omega} \mathcal{T}^\omega(-\omega, -\mathbf{q}, \theta') \\ &= \nu^2 Z^4 \mathcal{T}_0^2 \frac{v^2 q^2}{\omega^2} \oint \frac{d\theta d\theta'}{(2\pi)^2} \Gamma^\omega(\theta - \theta') \cos \theta \cos \theta' \\ &= \frac{\nu v^2 q^2}{2 \omega^2} \nu Z^2 \oint \frac{d\theta}{2\pi} \Gamma^\omega(\theta) \cos \theta. \end{aligned} \quad (21)$$

The terms $\Pi_{n \geq 3}$, expanded in qv/ω , yield contributions which are higher order in q . The same is true for contributions arising from expanding \mathcal{T}^ω , Γ^ω in powers of \mathbf{q} and ω (with the exception for potentially relevant linear terms \mathcal{T}_1 , \mathcal{T}_2 in Eq.(19) which merely cancel out). These terms are therefore not essential in the long-wavelength limit. Combining all the above results for Π_0 and $\Pi_{n \geq 1}$, we find the long-wavelength asymptotic behavior for the net polarization function:

$$\Pi(\mathbf{q}, \omega) = \frac{1}{2} \nu (1 + F_1) \frac{v_F^2 q^2}{\omega^2}, \quad (22)$$

$$F_1 = \nu Z^2 \oint \frac{d\theta}{2\pi} \Gamma^\omega(\theta) \cos \theta. \quad (23)$$

The quantity F_1 also represents an eigenvalue of the integral operator \hat{F} corresponding to eigenvectors $\cos \theta$ and $\sin \theta$. We can write $F_1 = \hat{F}[\cos \theta]$, which gives a Fourier harmonic of the operator kernel identical to Eq.(23).

Plasmon dispersion can now be obtained from the relation $1 - V(q)\Pi(q, \omega) = 0$, giving Eq.(2). The effects of interaction between fermions are ‘‘encapsulated’’ in the quantity Y which equals Fermi velocity v_0 in the absence of interactions and is renormalized to a different value in an interacting system.

We note a subtle difference between the quantities F_m used in the FL literature¹⁴ and those used here. The distinction arises due to the long-range character of the $1/r$ interaction. In our case the density-density interaction $F(\theta - \theta')$ accounts for the effects due to exchange correlation but not for the Hartree effects. The Hartree contribution is expressed through the $1/r$ interaction taken at the plasmon momentum \mathbf{q} , corresponding to the Feynman graphs which can be disconnected by cutting a single interaction line. These contributions are incorporated in the dynamically screened interaction, Eq.(8), and hence not included in the definition of Γ^ω above. This difference manifests itself in the sign of the interaction parameters. In Fermi liquids with short-range interactions, the Landau parameters describing density-density response are dominated by the Hartree effects. As a result, they have positive sign for weak repulsive interactions. In contrast, our F_m are negative, since they are dominated by exchange effects. In particular, we expect $F_1 < 0$. The negative sign, expected from this general argument, is also borne out by a microscopic analysis at weak coupling, see below.

We also note an interesting analogy between the approach developed in this section and the analysis of superconducting Fermi liquids by Larkin and Migdal,²¹ and Leggett.²² Refs.21,22 were concerned with Fermi-liquid renormalization of the quantities such as superfluid density in a metal with BCS pairing. Their analysis focused on the current correlation function which determines the response of current to vector potential, and followed similar steps as in the above discussion of $\Pi(\mathbf{q}, \omega)$. The renormalization effects were expressed through a combination of FL parameters, featuring a cancellation for a system with a parabolic band.

II. DENSITY DEPENDENCE FROM ONE-LOOP RG

In this section we derive plasmon dispersion for a simple model describing strongly interacting Dirac particles. This is done by employing the renormalization group analysis developed in Refs.¹⁶⁻¹⁸. We treat the Coulomb interaction which mediates two-body scattering by accounting for dynamical screening in the random-phase approximation (RPA), giving

$$U_{\mathbf{q}, \omega} = \frac{V(\mathbf{q})}{\epsilon(\mathbf{q}, \omega)}, \quad \epsilon(\mathbf{q}, \omega) = 1 - V(\mathbf{q})\Pi(\mathbf{q}, \omega). \quad (24)$$

Here the quantity $\epsilon(\mathbf{q}, \omega)$ which describes dynamical screening is identical to that introduced in the above discussion of the dynamical density correlator, Eq.(8). Here $\Pi(\mathbf{q}, \omega)$ is the polarization function²

$$\Pi(\mathbf{q}, \omega) = N \sum_{\mathbf{k}, s, s'} |F_{\mathbf{k}, \mathbf{k}+\mathbf{q}}|^2 \frac{f(\epsilon_{\mathbf{k}, s}) - f(\epsilon_{\mathbf{k}+\mathbf{q}, s'})}{i\omega + \epsilon_{\mathbf{k}, s} - \epsilon_{\mathbf{k}+\mathbf{q}, s'} + i0}, \quad (25)$$

with the band indices $\{s, s'\} = \pm$ and the coherence factors $|F_{\mathbf{k}, \mathbf{k}'}|^2 = |\langle \mathbf{k}', s' | \mathbf{k}, s \rangle|^2$ describing overlaps of different pseudospin states. The polarization function is a sum of interband and intraband contributions, $\Pi = \Pi_1 + \Pi_2$, described by $s' \neq s$ and $s' = s$, respectively. The factor $\epsilon(\mathbf{q}, \omega)$ describes the effect of intrinsic screening in graphene arising due to both the interband and intraband polarization. Below we give expressions that will be used in our analysis (for a comprehensive treatment of the quantity $\Pi(\mathbf{q}, \omega)$ we refer to Ref.2). For undoped graphene, only interband transitions contribute, giving $\Pi_1(\mathbf{q}, \omega) = -\frac{N}{16} \frac{\mathbf{q}^2}{\sqrt{v^2 \mathbf{q}^2 + \omega^2}}$. This dependence is key for RG analysis.¹⁶⁻¹⁸

The full RPA analysis of log-divergent corrections to Greens functions and vertices was performed in Refs.¹⁶⁻¹⁸. Below we show the results for one-loop RG calculation for large N , the results for $N \sim 1$ are qualitatively similar, however the mathematical expressions are more cumbersome. The renormalization group flow for the velocity takes the form

$$\frac{dv}{d\ell} = \beta v, \quad \beta = \frac{8}{N\pi^2}, \quad (26)$$

where $\ell = \ln(p_0/p)$ is the RG time parameter (here the UV cutoff is set by interatomic spacing in graphene lattice, $p_0 \sim a^{-1}$). This gives a power-law dependence

$$v(p) = (p/p_0)^{-\beta} v_0. \quad (27)$$

For $N = 4$ we find $\beta \approx 0.2$. This value is obtained from a one-loop RG which employs $1/N$ as a small parameter. Acknowledging an approximate character of the scaling dimensions obtained from one-loop RG, we shall leave the exponent β unspecified in the analytic expressions.

In the case of interest (doped graphene) the interband contribution Π_1 follows the above dependence for large

momenta and frequencies, $|\mathbf{q}| \gg p_F$, $\omega \gg E_F$, which provide dominant contribution to the RG flow of various quantities. The intraband contribution Π_2 is much smaller than Π_1 at large energies and momenta, however these two contributions are comparable for $|\mathbf{q}| \sim p_F$, $\omega \sim E_F$. In the static limit, $\omega \ll E_F$, the polarization is dominated by the Π_2 contribution. In the range $q < 2p_F$, which is where we will need it below, it is identical to that for two-dimensional systems with parabolic band,

$$\Pi(|\mathbf{q}| < 2p_F) = -N\nu, \quad (28)$$

$\nu = p_F/2\pi v$ (we refer to Ref.2 for the analysis of other regimes). This gives a standard expression for the static RPA-screened interaction

$$U_{\mathbf{q},0} = \frac{2\pi e^2}{\kappa|\mathbf{q}| + 2\pi N\nu e^2} \quad (29)$$

We can obtain the two-particle scattering vertex Γ^ω by taking the interaction on the Fermi surface, $\mathbf{q} \sim p_F$, $\omega \ll E_F$. This gives

$$\Gamma^\omega(\theta, \theta') = -g_{\mathbf{p},\mathbf{p}'} [\mathcal{T}(\Delta\mathbf{p})]^2 U_{\Delta\mathbf{p},0}, \quad \Delta p = 2p_F \sin \frac{\Delta\theta}{2}, \quad (30)$$

where $g_{\mathbf{p},\mathbf{p}'} = |\langle \mathbf{p}' | \alpha' | \mathbf{p} \alpha \rangle|^2 = \cos^2(\Delta\theta/2)$ is the coherence factor describing the overlap of (pseudo)spinors describing quasiparticles at different points of the Fermi surface (here $\Delta\theta = \theta - \theta'$). The minus sign in Eq.(30) arises because this expression represents a contribution from an exchange part of the two-particle vertex.¹⁴

Landau parameters can now be obtained from the relation between the Landau functional and the vertex Γ^ω , Eq.(18). Combining Eq.(18) and Eq.(30), we find

$$F(\theta - \theta') = -\nu g_{\mathbf{p},\mathbf{p}'} Z^2 [\mathcal{T}(\Delta\mathbf{p})]^2 U_{\Delta\mathbf{p},0} \quad (31)$$

In the large N limit, the static RPA-screened interaction can be approximated as $U_{\mathbf{q},\omega} \approx -\frac{1}{\Pi(\mathbf{q},\omega)} = \frac{1}{N\nu}$, where we take into account that $|\Delta p| < 2p_F$.

Both Z and \mathcal{T} flow under RG, however their product remains equal to unity because of the Ward identity. As a result, the Landau function does not undergo power-law renormalization. Starting from $Z(p)\mathcal{T}(p) = 1$, where both $Z(p)$ and $\mathcal{T}(p)$ are given by power laws drawn from RG, we set $p = p_F$. This gives

$$F(\theta - \theta') = -\frac{1}{N} \left(\frac{\mathcal{T}(\Delta\mathbf{p})}{\mathcal{T}(p_F)} \right)^2 \cos^2 \left(\frac{\theta - \theta'}{2} \right). \quad (32)$$

Up to a remnant dependence on p_F which may arise in the angle dependence due to the ratio $\mathcal{T}(\Delta\mathbf{p})/\mathcal{T}(p_F)$, the function F does not flow under RG.

While the function $F(\theta - \theta')$ is essentially independent of doping, the velocity has a power-law dependence on doping, $v \propto p_F^{-\beta}$. Combining these results, we find a power law dependence for plasmon dispersion,

$$\omega^2 = A|\mathbf{q}|, \quad A = \frac{N e^2 p_F v(p_F)}{2\kappa \hbar^2} (1 + F_1) \propto p_F^{1-\beta}, \quad (33)$$

where v vs. p dependence is given by Eq.(27). This result is valid for plasmons with long wavelengths, $q \ll p_F$. The predicted power-law dependence of plasmon on carrier concentration holds for both large and small densities, except very near the neutrality point where spatial inhomogeneity and thermal broadening start playing a role. Plasmons tend to stiffen due to RG-enhancement of velocity, and to soften due to the negative sign of F_1 . However, since F_1 does not flow under RG, whereas velocity v does, the net effect of interactions leads to stiffening of plasmon dispersion. The predicted dependence $A \propto n^{(1-\beta)/2}$ can be used for extracting the exponent β from measurement results.

III. MAGNETOPLASMON IN A FERMI LIQUID

Below we will treat plasmons using Landau's transport equations, presenting the derivation in a way that will help to make connection to the microscopic derivation in Sec.I. We will first deal with plasmons in the absence of magnetic field, then proceed to add a B field. Some of the relevant quantities, such the Landau FL interaction $F(\theta - \theta')$ has already been introduced and analyzed, here we re-introduce and discuss them again in the framework of Landau FL transport equation.

In Landau's semiclassical framework, the fundamental effect dominating the Fermi-liquid behavior is forward scattering wherein the whole system of interacting particles acts as a refractive medium which makes each quasiparticle energy a function of occupancies of other particles. This is described by so-called Landau functional,

$$\delta\epsilon(\mathbf{p}) = \int \frac{d^2 p'}{(2\pi)^2} f(\mathbf{p}, \mathbf{p}') \delta n(\mathbf{p}', \mathbf{r}), \quad (34)$$

where $\delta n(\mathbf{r}, t)$ accounts for deviation of quasiparticle distribution from equilibrium.

Since deviation from equilibrium occurs in a narrow band of states near Fermi surface, it is convenient to write the Landau functional by setting $|\mathbf{p}| = |\mathbf{p}'| = p_F$ and parameterizing the Fermi surface by a unit vector $\mathbf{n} = \mathbf{p}/|\mathbf{p}|$. Introducing the dimensionless Landau interaction $F(\mathbf{p}, \mathbf{p}') = \nu f(\mathbf{p}, \mathbf{p}')$, where $\nu = p_F/(2\pi \hbar^2 v)$ is the density of states per flavor, we obtain

$$\epsilon(\mathbf{p}, \delta n) = \epsilon_0(\mathbf{p}) + \int \frac{d\theta'}{2\pi} F(\mathbf{p}, \mathbf{p}') \delta \tilde{n}(\mathbf{p}', \mathbf{r}). \quad (35)$$

Here $\epsilon_0(\mathbf{p}) = v(p - p_F)$ is linearized quasiparticle energy, the angle θ' describes orientation of \mathbf{p}' , and $\delta \tilde{n}(\mathbf{p})$ is obtained by integrating $\delta n(\mathbf{p})$ along the Fermi surface normal. The expression (35) can be treated as a Hamiltonian of one quasiparticle moving in a selfconsistent field of other quasiparticles. The equation of motions can then be obtained from Hamiltonian formalism via $\partial_t n = \{H, n\}$. This gives

$$(\partial_t + \mathbf{v}\nabla)\delta n(\mathbf{p}, \mathbf{r}, t) = -\mathbf{v}\nabla \hat{F} \delta n(\mathbf{p}, \mathbf{r}, t), \quad (36)$$

where \widehat{F} is the integral operator defined in Eq.(35).

In a system with rotational symmetry, such as graphene and 2DEG's, the functional F depends only on the angle between \mathbf{p} and \mathbf{p}' :

$$\widehat{F}\delta n(\theta) \rightarrow \oint \frac{d\theta'}{2\pi} F(\theta - \theta')\delta n(\theta') \quad (37)$$

This expression defines a hermitian operator in the space of functions on the Fermi surface with the inner product

$$\langle f_1(\theta)|f_2(\theta)\rangle = \oint \frac{d\theta}{2\pi} f_1^*(\theta)|f_2(\theta). \quad (38)$$

The eigenvalues of \widehat{F} are simply given by the Fourier coefficients

$$F_m = \overline{F(\theta)e^{-im\theta}} = \oint \frac{d\theta}{2\pi} F(\theta)e^{-im\theta}. \quad (39)$$

The quantities F_m represent the Landau interaction constants of a 2D FL system.

To describe plasmons and relate their dispersion with the quantities F_m we add to Eq.(36) a long range electric field arising due to oscillating charge density,

$$\left(\partial_t + \mathbf{v}\nabla(\widehat{1} + \widehat{F})\right)\delta n(\mathbf{p}, \mathbf{r}, t) + e\mathbf{E}\nabla_{\mathbf{p}}n_0(\mathbf{p}) = 0 \quad (40)$$

where $n_0(\mathbf{p})$ is the equilibrium Fermi distribution. Here $\mathbf{E} = -\nabla\Phi$, where $\Phi(\mathbf{r})$ is the potential

$$\Phi(\mathbf{r}) = \sum_i \int d^2r' \oint \frac{d\theta'}{2\pi} \frac{e}{\kappa|\mathbf{r} - \mathbf{r}'|} \delta n(\theta', \mathbf{r}', t).$$

Here the sum is taken over N spin/valley flavors, and the dielectric constant κ accounts for screening by substrate. Performing Fourier transform, $\delta n(\theta, \mathbf{r}, t) = \int \int \frac{d\omega d^2k}{(2\pi)^3} \delta n_{\omega, \mathbf{q}}(\theta)e^{-i\omega t + i\mathbf{q}\mathbf{r}}$, we arrive at an eigenvalue equation of the form identical to that found in Sec.I by analyzing poles of the dynamical screening function,

$$1 - V(\mathbf{q})\Pi(\mathbf{q}, \omega) = 0 \quad (41)$$

The quantity $\Pi(\mathbf{q}, \omega)$ is identical to that found above by summation of FL-type ladder graphs,

$$\Pi(\mathbf{q}, \omega) = N\nu \text{Tr}_{\theta} \left(\frac{1}{\omega - \mathbf{q}\mathbf{v}(1 + \widehat{F})} \mathbf{q}\mathbf{v} \right) \quad (42)$$

where trace is taken with respect to the inner product defined by Eq.(38).

Plasmon dispersion in the long wavelength limit can be found by expanding in the ratio $v|\mathbf{q}|/\omega$. We obtain

$$\Pi(\mathbf{q}, \omega) \approx \frac{\nu}{\omega^2} \langle \mathbf{q}\mathbf{v} | (1 + \widehat{F}) | \mathbf{q}\mathbf{v} \rangle = \frac{\nu q^2 v^2}{\omega^2} \langle \cos\theta | (1 + \widehat{F}) | \cos\theta \rangle \quad (43)$$

Expressing the angle-averaged quantity through the Fourier coefficient F_1 and using the relation $\nu = p_F/(2\pi v)$ we rewrite this result as

$$\Pi(\mathbf{q}, \omega) = \frac{N p_F \mathbf{q}^2}{4\pi\omega^2} v(1 + F_1) \quad (44)$$

Plugging this into Eq.(41) and restoring Planck's constant, we obtain the same expression for plasmon dispersion as above, see Eq.(2).

This analysis can be easily generalized to a system in the presence of an external magnetic field. This is done by accounting for the Lorentz force in the $\nabla_{\mathbf{p}}n$ term:

$$\left(\partial_t + \mathbf{v}\nabla(\widehat{1} + \widehat{F})\right)\delta n(\mathbf{p}, \mathbf{r}, t) + \left(e\mathbf{E} + \frac{e}{c}\tilde{\mathbf{v}} \times \mathbf{B}\right) \cdot \nabla_{\mathbf{p}}n = 0 \quad (45)$$

where the velocity $\tilde{\mathbf{v}} = \nabla_{\mathbf{p}}\epsilon(\mathbf{p}, \delta n)$ includes contributions due to the distribution function $\delta n(\mathbf{p})$. This equation can be linearized as above, $n(\mathbf{p}, \mathbf{r}, t) = n_0(\mathbf{p}) + \delta n(\mathbf{p}, \mathbf{r}, t)$. In doing so, particular caution must be taken with the Lorentz force term since it is affected by the FL interactions. Accounting for the term in the velocity $\tilde{\mathbf{v}}$ that depends on $\delta n(\mathbf{p})$, we write

$$\begin{aligned} \tilde{\mathbf{v}}(n_0 + \delta n) &= \partial_{\mathbf{p}}\epsilon(n_0 + \delta n) \\ &= \partial_{\mathbf{p}}\epsilon + \partial_{\mathbf{p}}\widehat{F}\delta n = \mathbf{v} + \widehat{F}\partial_{\mathbf{p}}\delta n, \end{aligned} \quad (46)$$

Here we used Eq.(35) and on the last step performed integration by parts.

Terms linear in δn can arise both from $\nabla_{\mathbf{p}}n_0$ and $\tilde{\mathbf{v}}$. Taking a solution in a plane wave form $\delta n(\mathbf{r}, \mathbf{p}, t) \propto e^{-i\omega t + i\mathbf{q}\mathbf{r}} \nabla_{\mathbf{p}}n_0(\mathbf{p})f(\theta)$ we have

$$\begin{aligned} \left(i\omega - ivq \cos\theta(1 + \widehat{F})\right)f(\theta) - \frac{e}{c}(\mathbf{v} \times \mathbf{B}) \cdot \nabla_{\mathbf{p}}f(\theta) \\ - \left(\widehat{F}\nabla_{\mathbf{p}}f(\theta) \times \mathbf{B}\right) \cdot \mathbf{v} = ivV(q)qv \cos\theta \oint \frac{d\theta'}{2\pi} f(\theta') \end{aligned} \quad (47)$$

where θ is the angle between \mathbf{q} and \mathbf{v} . This equation can be simplified as follows:

$$\begin{aligned} \left(i\omega - ivq \cos\theta(1 + \widehat{F}) - \omega_B(1 + \widehat{F})\partial_{\theta}\right)f(\theta) \\ = ivV(q)qv \cos\theta \oint \frac{d\theta'}{2\pi} f(\theta'), \quad \omega_B = \frac{evB}{p_Fc}. \end{aligned} \quad (48)$$

This is an eigenvalue problem with ω a spectral parameter and $f(\theta)$ an eigenfunction. Inverting the operator on the left hand side gives a self-consistency equation

$$\oint \frac{ivV(q)qv}{\omega + i\omega_B(1 + \widehat{F})\partial_{\theta} - qv \cos\theta(1 + \widehat{F})} \cos\theta \frac{d\theta}{2\pi} = 1,$$

Magnetoplasmon dispersion can be obtained via perturbation theory in the parameter $qv/\omega \ll 1$, giving

$$\omega^2(\mathbf{q}) = (1 + F_1)^2\omega_B^2 + (1 + F_1)\frac{1}{2}V(\mathbf{q})\nu\mathbf{q}^2v^2 \quad (49)$$

Using the notation $Y = (1 + F_1)v$ we arrive at Eq.(3). Magnetoplasmon dependence on interactions is described by the parameter Y identical to that found for plasmons at $B = 0$. The density dependence of the quantities v and $1 + F_1$ can be linked to their flow under RG. As discussed above, the power-law RG flow of velocity leads to stiffening of plasmon dispersion, which overwhelms the effect of softening due to the negative sign of F_1 .

To put the above results in perspective, we recall that there is a crucial difference between the effects of interaction in graphene and in electron systems with parabolic band, such as those realized in GaAs. As noted above, for particles with quadratic dispersion the effects of interaction disappear because of the Fermi-liquid identity that relates renormalized velocity with the quantity F_1 ,

$$Y = (1 + F_1)v = v_0 \quad (50)$$

where $v_0 = p_F/m$ is Fermi velocity for noninteracting particles. This identity, which follows from Galilean invariance, is peculiar to systems with quadratic dispersion and does not hold in graphene. As a result, plasmons in graphene depend in a nontrivial way on the Fermi ve-

locity value v which undergoes renormalization by the interaction effects, and also on the FL interaction via a factor $1 + F_1$. These quantities, as we have seen above, are directly related to plasmon dispersion. The dependence of plasmon frequency on carrier concentration is expected to follow $n^{1/4}$ power law for weakly interacting electrons. The deviation from this dependence essentially maps out theoretically predicted RG flow of $Y = (1 + F_1)v$, with the momentum dependence parameterized by p_F via the dependence on doping. This gives a unique opportunity to employ plasmon resonance as a probe of the RG theory of interaction effects in graphene.

We thank F. H. L. Koppens, I. V. Kukushkin and M. Yu. Reizer for useful discussions.

-
- ¹ B. Wunsch, T. Stauber, F. Sols, and F. Guinea, *New J. Phys.* **8**, 318 (2006).
- ² E. H. Hwang, and S. Das Sarma, *Phys. Rev. B*, **75** 205418 (2007).
- ³ M. Polini, A. H. MacDonald, and G. Vignale, preprint at <http://arXiv.org/abs/0901.4528> (2009).
- ⁴ S. Das Sarma and E. H. Hwang, *Phys. Rev. Lett.* **102**, 206412 (2009).
- ⁵ E. G. Mishchenko, A. V. Shytov, P. G. Silvestrov, *Phys. Rev. Lett.* **104**, 156806 (2010).
- ⁶ G. F. Giuliani, G. Vignale, *Quantum Theory of the Electron Liquid* (Cambridge Univ. Press, 2005).
- ⁷ T. N. Theis, *Surf. Sci.* **98**, 515-532 (1980).
- ⁸ A. V. Chaplik, *Surface Science Rep.* **5**, 289 (1985).
- ⁹ F. Bonaccorso, Z. Sun, T. Hasan, and A. C. Ferrari *Nat Photon.* **4**, 611-622 (2010).
- ¹⁰ F. H. L. Koppens, D. E. Chang, and F. J. Garcia de Abajo. *Nano Letters* **11**, 3370-3377 (2011).
- ¹¹ L. Ju, B. Geng, J. Horng, C. Girit, M. Martin, Z. Hao, H. A. Bechtel, X. Liang, A. Zettl, Y. R. Shen, and F. Wang, *Nature Nanotechnology* **6**, 630-634 (2011).
- ¹² J. Chen, M. Badioli, P. Alonso-Gonzalez, S. Thongrattanasiri, F. Huth, J. Osmond, M. Spasenovic, A. Centeno, A. Pesquera, P. Godignon, A. Zurutuza Elorza, N. Camara, F. J. Garcia de Abajo, R. Hillenbrand, and F. H. L. Koppens, *Nature* **487**, 77-81 (2012).
- ¹³ S. H. Abedinpour, G. Vignale, A. Principi, M. Polini, W.-K. Tse, A. H. MacDonald, *Phys. Rev. B* **84**, 045429 (2011).
- ¹⁴ E. M. Lifshitz and L. P. Pitaevskii, *Statistical Physics, Part 2*, (Pergamon Press, Oxford 1986).
- ¹⁵ A.V. Chaplik, *Zh. Eksp. Teor. Fiz.* **62**, 746 (1972) [*Sov. Phys. JETP* **35**, 395-398 (1972)].
- ¹⁶ J. González, F. Guinea, and M. A. H. Vozmediano, *Nucl. Phys. B* **424**, 595 (1994); *Phys. Rev. B* **59**, R2474 (1999).
- ¹⁷ O. Vafek, *Phys. Rev. Lett.* **98**, 216401 (2007).
- ¹⁸ D. T. Son, *Phys. Rev. B* **75**, 235423 (2007).
- ¹⁹ D. C. Elias, R. V. Gorbachev, A. S. Mayorov, S. V. Morozov, A. A. Zhukov, P. Blake, L. A. Ponomarenko, I. V. Grigorieva, K. S. Novoselov, F. Guinea, and A. K. Geim, *Nature Phys.* **7**, 701 (2011).
- ²⁰ P. Nozières and J. M. Luttinger, *Phys. Rev.* **127**, 1423 (1960).
- ²¹ A. I. Larkin and A. B. Migdal, *Zh. Eksperim. i Teor. Fiz.* **44**, 1703 (1963) [English transl: *Soviet Phys. JETP* **17**, 1146 (1963)].
- ²² A. J. Leggett, *Phys. Rev.* **A140**, 1869 (1965).